Journal of Materials Chemistry

Cite this: J. Mater. Chem., 2012, 22, 9957

www.rsc.org/materials

PAPER

Photoluminescence investigations on a novel green-emitting phosphor $Ba_3Sc(BO_3)_3:Tb^{3+}$ using synchrotron vacuum ultraviolet radiation

De-Yin Wang,[a] Yi-Chin Chen,[a] Chien-Hao Huang,[a] Bing-Ming Cheng[b] and Teng-Ming Chen*[a]

Received 5th December 2011, Accepted 19th March 2012
DOI: 10.1039/c2jm16350k

Vacuum ultraviolet (VUV) spectroscopic properties of undoped and Tb^{3+}-doped $Ba_3Sc(BO_3)_3$ were investigated by using synchrotron radiation. The Tb^{3+}-doped $Ba_3Sc(BO_3)_3$ sample crystallized in a flower-like shape even was synthesized at 1100 °C. Upon VUV excitation, $Ba_3Sc(BO_3)_3$ exhibited an intrinsic broad UV emission centered at 336 nm, which results from radiative annihilation of self-trapped exciton (STE) that may presumably be associated with band-gap excitations or molecular transitions within the BO_3^{3-} group. The maximum host absorption for $Ba_3Sc(BO_3)_3$ was found at about 180 nm. Upon doping of Tb^{3+} ions into $Ba_3Sc(BO_3)_3$, an efficient energy transfer from the host excitations to Tb^{3+} *via* STE emission was observed, showing host sensitization of Tb^{3+} occurs. The energy transfer from host to Tb^{3+} *via* STE emission in $Ba_3Sc(BO_3)_3:Tb^{3+}$ was studied as a function of temperature and Tb^{3+} doping concentration. It has been demonstrated that the energy transfer efficiency was increased with either increasing temperature or Tb^{3+} doping concentration. In the case of temperature dependent energy transfer, the energy transfer from the STE to Tb^{3+} is thermally activated, probably due to exciton mobility, while in the case of concentration dependent energy transfer, the energy transfer from the STE to Tb^{3+} is promoted due to a closer distance between the STE and Tb^{3+} at high Tb^{3+} concentration.

1 Introduction

With the rapid development of mercury-free fluorescent lamps and plasma display panels (PDPs), which use Xe-discharge as the excitation source for phosphor, the demand for phosphors that could be efficiently excited by a vacuum ultraviolet (VUV, $\lambda <$ 200 nm) radiation has been rapidly increasing.[1–11] Several VUV phosphors have been developed for PDPs applications, such as red-emitting $(Y,Gd)BO_3:Eu^{3+}$, blue-emitting $BaMgAl_{10}O_{17}:Eu^{2+}$ and green-emitting $Zn_2SiO_4:Mn^{2+}$.[11–14] However, many problems still remain, including poor color purity for the red phosphor, thermal and aging degradation for the blue phosphor, and long decay time for the green phosphor.[11–14] In order to improve the performance of PDPs, much attention has been paid to explore and find new color-emitting phosphors. In the case of phosphors excited by VUV radiation, it is widely considered the excitation energy is transferred from host matrix to the activator;[15,16] that is to say, the activator is not directed excited. As a consequence, for a good VUV phosphor, it is necessary for the excitation energy to be efficiently transferred from the host matrix to the activator. If a host itself emits and its emission overlaps with the direct absorptions of an activator (*e.g.*, *f–f* or *f–d* transition), then nonradiation energy transfer from host to activator would happen according to the Forster–Dexter energy transfer theory,[17] giving rise to efficient emission from activator in such host. From this standpoint, with an aim to develop new green-emitting phosphor, we have selected $Ba_3Sc(BO_3)_3$ as a host lattice with Tb^{3+} serving as an activator. The choice of $Ba_3Sc(BO_3)_3$ is motivated by previous results that several of its isostructural compounds such as $Ba_3Y(BO_3)_3$ and $Ba_3Lu(BO_3)_3$ exhibit intrinsic UV emission under X-ray excitation.[18] In addition, the *f–f* and *f–d* transitions of Tb^{3+} generally located in the UV region. Therefore, due to spectra overlap, efficient host-to-Tb^{3+} energy transfer is expected in Tb^{3+}-doped $Ba_3Sc(BO_3)_3$. In this paper, we have investigated the energy transfer from the host excitations to Tb^{3+} in the matrix of $Ba_3Sc(BO_3)_3$, and examined the influence of temperature and Tb^{3+} doping concentrations on the energy transfer process.

2 Experimental

2.1. Materials and synthesis

Powder samples of undoped and Tb^{3+}-doped $Ba_3Sc(BO_3)_3$ (BSB) were synthesized by high temperature solid-state reactions. $BaCO_3$ (99.9%, Sigma-Aldrich), H_3BO_3 (99.99%, Sigma-Aldrich), Sc_2O_3 (99.9%, Aldrich) and Tb_4O_7 (99.9%, Aldrich) were used as reagents. The oxides were mixed according to the desired stoichiometric ratios of each sample, and then

[a]Phosphors Research Laboratory and Department of Applied Chemistry, National Chiao Tung University, Hsinchu 30010, Taiwan. E-mail: tmchen@mail.nctu.edu.tw; Tel: + 886-35731695
[b]National Synchrotron Radiation Research Center, Hsinchu 30076, Taiwan

thoroughly ground. The obtained mixtures were fired at 1100 °C in a reducing atmosphere (15% H_2/85% Ar) for the Tb^{3+}-doped samples and in air for the undoped sample.

2.2. Characterization methods

The phase purity of all samples was checked by using powder X-ray diffraction (XRD) analysis with a Bruker AXS D8 advanced automatic diffractometer operated at 40 kV and 40 mA with Cu-Kα radiation ($\lambda = 1.5418$ Å). Particle sizes and shapes were determined by a scan electron microscope (SEM) (JSM-6390LV, JEOL).

The VUV photoluminescence (PL) spectra were recorded at the Beamline 03A at National Synchrotron Radiation Research Center (NSSRC) in Taiwan. The experimental setup for PL spectra was similar to that described elsewhere.[2,19] In summary, VUV excitation light from this high-flux beamline attached to the 1.5-GeV storage ring was dispersed with a six-meter cylindrical grating monochromator (CGM). The intensity of the VUV light is monitored with a gold mesh transmitting about 90% and recorded with an electrometer (Keithley 6512). A Jobin-Yvon HR320 equipped with a 1200 lines/mm grating and a Hamamatsu R943-02 photomultiplier (PMT) were used to record the PL spectra. For measurement of PL excitation (PLE) spectra, the dispersive emission was monitored at selected band; in which, the CGM beam line with a 450 lines/mm grating was scanned. All the PLE spectra were normalized with the spectral response curve of the CGM beam line. For measurements of low temperature spectra, the sample holder was attached to a cryo-head of a helium closed-cycle cryostat system (APD HC-4); which was mounted on a rotatable flange so that the sample could be rotated to about 45° with respect to both the incident VUV source and the entrance slit of the dispersed monochromator. The temperature control unit provided the cold head of the cryostat to better than ±1 K during the data collection period. Unless otherwise specified, all spectra were measured at room temperature.

3 Results and discussion

3.1 Crystal structure, phase identification and microstructure

$Ba_3Sc(BO_3)_3$ (BSB) crystallizes in hexagonal crystal structure with space group $P6_3cm$. Its crystal structure is built with isolated BO_3 triangles and scandium–oxygen octahedra and barium–oxygen nine-vertex polyhedra.[20] All boron atoms are coordinated to three oxygen atoms, which are distributed layer upon layer along the c-axis. In the crystal structure of $Ba_3Sc(BO_3)_3$, there are two non-equivalent Sc sites having C_3 and C_{3v} point symmetries and four different Ba sites having C_{3v}, C_s, C_3 and C_s point symmetries, respectively.[20] Shown in Fig. 1 are the XRD patterns of the undoped and Tb^{3+} doped BSB. The XRD patterns of the synthesized samples BSB:xTb^{3+} ($0 \le x \le 20\%$) are in good agreement with reference data (ICSD No.75340) regardless of Tb^{3+} doping concentration, indicating that these Tb^{3+} doped samples retained the same crystal structure as that of the undoped BSB. However, when Tb^{3+} doping concentration is increased to 30% (see Fig. 1), some new peaks marked by the asterisk appear, which probably be ascribed to the formation of $Ba_3Tb(BO_3)_3$ (PDF No. 511848), so in this work only samples

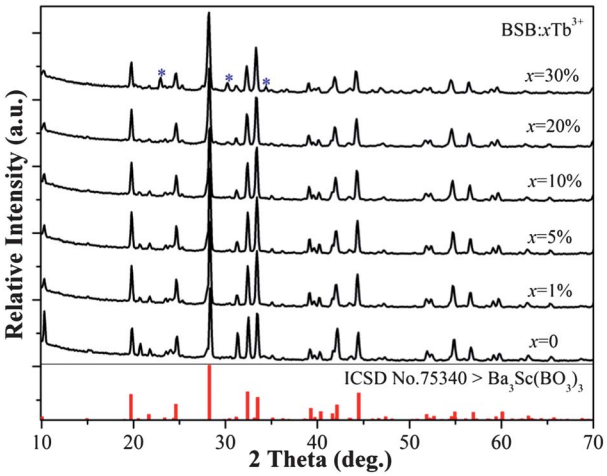

Fig. 1 XRD patterns of BSB:xTb^{3+}($0 \le x \le 30\%$).

with composition BSB:xTb^{3+} ($0 \le x \le 30\%$) were investigated. Fig. 2 shows the SEM image of a 20% Tb-doped BSB sample that has flower-liked shape with average diameter around 6 μm. Each flower consists of dozens of petals with the averages width of 200 nm and length of 2 μm. Taking a close look at a single flower (see the inset in Fig. 2), we can see that all the petals grow out from the central part of a flower and look like icicles.

3.2 VUV-excited spectral properties of undoped and Tb^{3+}-doped BSB

The VUV spectroscopic investigation of undoped BSB was performed as a prerequisite for the interpretation of luminescence spectra of BSB:Tb^{3+}. The PL and PLE spectra of the undoped BSB measured at room temperature are shown in Fig. 3. Upon excitation at 172 nm, BSB emits a broad intrinsic UV-luminescence band with maximum at 336 nm. The emission band most likely arises from the recombination of self-trapped excitons (STE) that may be associated with band-gap excitations or molecular transitions within the BO_3^{3-} group.[21,22] The broad absorption band with maximum at round 180 nm in the PLE spectrum of BSB, obtained by monitoring the intrinsic UV

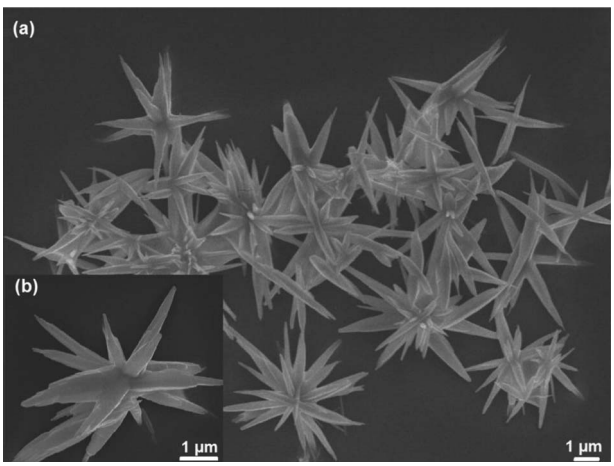

Fig. 2 SEM image of BSB:20%Tb^{3+}. The inset shows a zoomed image.

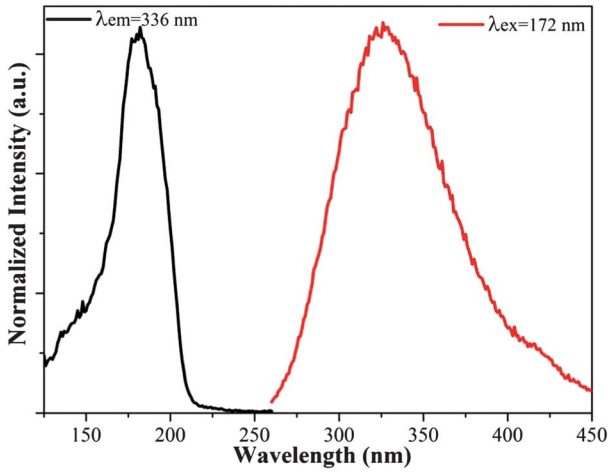

Fig. 3 PLE and PL spectra of undoped BSB monitoring the STE emission at 336 nm and under excitation at 172 nm.

emission, is assigned to the host absorption that could be associated with intramolecular transitions of the borate group. The intrinsic host emission has extended to 450 nm in wavelength, which partially overlaps with the Tb^{3+} 4*f*–4*f* absorptions (*e.g.*, $^7F_6 \rightarrow {}^5D_3$ transition). Due to the spectral overlap, when Tb^{3+} ions are introduced to the host lattice of BSB, efficient energy transfer from host excitation to Tb^{3+} ions is expected. Indeed, as indicated in Fig. 4, when BSB is doped with 1% Tb^{3+}, the intrinsic UV emission is greatly reduced and accompanied by an increase in Tb^{3+} emission, suggesting efficient energy transfer from STE to Tb^{3+}. The PL spectrum of the sample containing 1% Tb^{3+} can be divided into two spectral regions, an UV emission in 300–400 nm region ascribed to the overlapped emission from the host and Tb^{3+} $^5D_3$–$^7F_6$ transition, and a green emission in 475–650 nm region originated from Tb^{3+} $^5D_4$–^7F_J ($J = 6$, 5, 4 and 3) transitions. Weak $^5D_3$–$^7F_6$ transition of Tb^{3+} around 380 nm can be observed in the PL spectra of BSB:1%Tb^{3+}, implying that energy transfer from host to Tb^{3+} involves in Tb^{3+} $^5D_3$ state. Furthermore, Fig. 5 is a comparison between the PLE spectrum of BSB:1%Tb^{3+} obtained by monitoring the Tb^{3+} $^5D_4$–$^7F_5$ emission at 543 nm and that of undoped BSB monitoring the STE emission, respectively. The PLE spectrum of the two samples exhibits similarly features with a broad absorption band below 210 nm, indicating that they both resulted from the same origin, *viz*. host absorption. The presence of the host absorption band in the PLE spectrum of 1% Tb^{3+}-doped BSB, detecting within the Tb^{3+} emission, gives another evidence that the host-to-Tb^{3+} energy transfer in fact took place. Furthermore, as to the PLE spectrum of 1% Tb^{3+} doped sample, the strong excitation band in 220–270 nm region with maximum around 246 nm is assigned to the spin-allowed $4f^8$–$4f^75d^1$ transition of Tb^{3+}, and relative weak excitation band around 278 nm is assigned to the spin-forbidden $4f^8$–$4f^75d^1$ transition of Tb^{3+}.

3.3 Concentration-dependent luminescence of BSB:Tb^{3+}

To give further evidence to support the occurrence of host-to-Tb^{3+} energy transfer, and determine the optimal Tb^{3+}doping concentration in BSB:Tb^{3+}, concentration dependent luminescence measurements were performed. Presented in Fig. 6 are the PL spectra of BSB:$x$$Tb^{3+}$ ($0 \leq x \leq 30\%$) under excitation with light lying within the host absorption bands. As revealed in Fig. 6, in the presence of Tb^{3+}, the STE emission is greatly quenched due to energy transfer. At lower Tb^{3+} doping concentration (*i.e.*, 1%), weak STE emission can still be observed, because in this case a portion of excited STE could relax by photon emission. However, at higher Tb^{3+} doping concentration, the STE emission is significantly quenched. The energy transfer is so efficient that the STE emission almost totally quenched when Tb^{3+} doping concentration is increased to 5%. Assuming that the decrease of STE is caused by energy transfer from STE to Tb^{3+} acceptor only, and ignoring the possible energy transfer to other impurity or defect sites, we can roughly estimate the energy transfer efficiency (η) by analogy to the case for Ce^{3+}-Tb^{3+}:[23]

$$\eta = 1 - I_s/I_{s0} \quad (1)$$

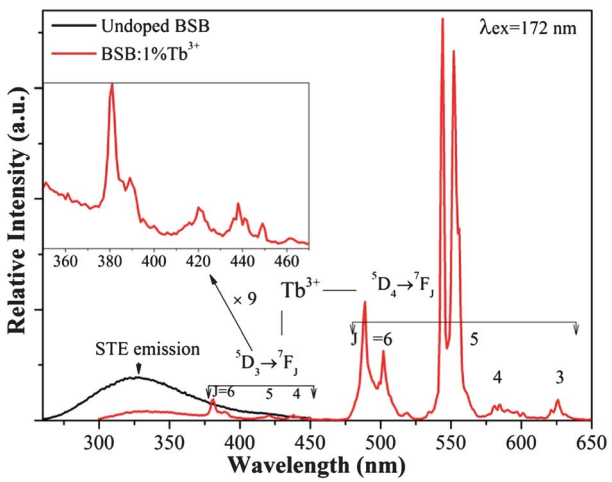

Fig. 4 PL spectra of undoped BSB and 1% Tb^{3+}-doped BSB under excitation at 172 nm. The inset shows an enlarged portion of the PL spectrum of BSB:1%Tb^{3+} in the 350–470 nm region.

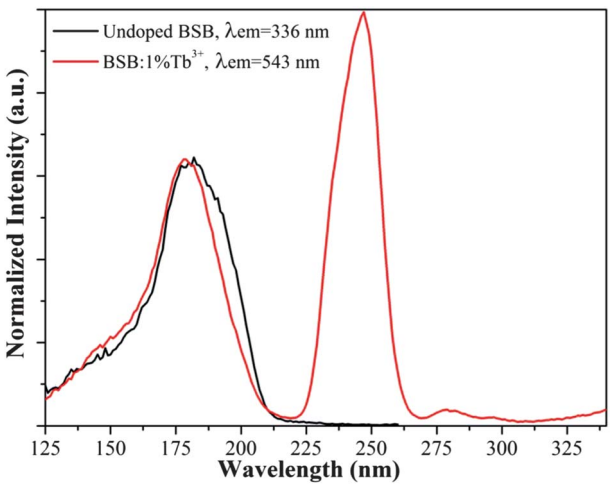

Fig. 5 PLE spectra of 1% Tb^{3+}-doped BSB monitoring Tb^{3+} emission at 543 nm and the STE emission of undoped BSB at 336 nm. The PLE spectra are normalized on the host absorption intensity.

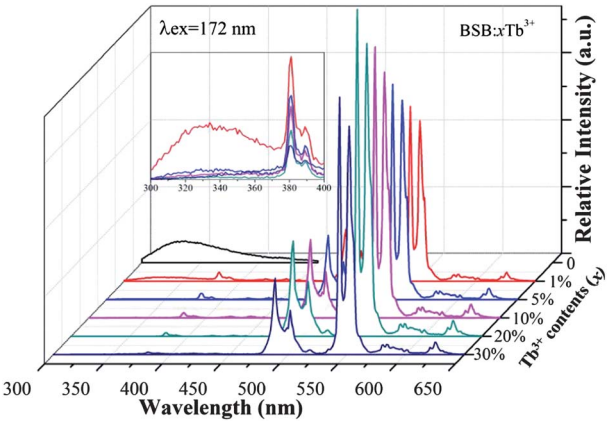

Fig. 6 Comparison of PL spectra of BSB:xTb^{3+} ($0 \leq x \leq 30\%$) under excitation at 172 nm. The inset shows an enlarged portion for the PL spectra of BSB:xTb^{3+} ($1 \leq x \leq 30\%$) in the 300–400 nm region.

where I_s and I_{s0} are the STE emission intensity in the presence and absence of Tb^{3+} acceptor, respectively. According to eqn (1), the energy transfer efficiency for 1% Tb^{3+}-doped sample is roughly estimated to be about 75%. With further increasing Tb^{3+} doping concentration, the corresponding STE emission intensity deceases further, and accordingly, the energy transfer efficiency at high Tb^{3+} doping concentration will be much greater than 75% and close to 100%. As the Tb^{3+} doping concentration increases, there are more Tb^{3+} ions that will be distributed around the created STE and the distance between the center of STE and Tb^{3+} is shortened and, consequently, thus the energy transfer probability between them is increased, then the STE emission is quenched. Partially owing to the host-to-Tb^{3+} energy transfer, it is found that the emission from Tb^{3+} $^5D_4$ level increases upon increasing Tb^{3+} dopant concentrations. In principle, an increasing in the Tb^{3+} concentration will increase its absorption efficiency, which will simultaneously increase the emitted light intensity of Tb^{3+}.[24] The optimal Tb^{3+} doping concentration in BSB:Tb^{3+} was found to be 20%. Upon 172 nm excitation, the relative quantum efficiency of the 20% Tb^{3+} doped sample was estimated to be about 39% by comparing its PL spectrum with that of sodium salicylate whose quantum efficiency is about 58% over the excitation wavelength range from 140 to 320nm.[21] With further increasing Tb^{3+} concentration, the Tb^{3+} $^5D_4$ emission starts to decease due to concentration quenching effect. In addition, it is found that the Tb^{3+} $^5D_3$–$^7F_6$ emission (~380 nm) is deceased with increasing Tb^{3+} dopant concentration (see the inset in Fig. 6), which is caused by the cross relaxation process between $^5D_3$, $^7F_0$ → $^5D_4$, $^7F_6$ levels.[11,25] An increasing in Tb^{3+} doping concentration has also shorten the distance between two adjacent Tb^{3+} ions, resulting in an increase in the cross relaxation probability; thus the Tb^{3+} $^5D_3$–$^7F_6$ emission is greatly reduced at high Tb^{3+} concentration.

3.4 Temperature-dependent luminescence of BSB:Tb^{3+}

To obtain a better insight in the energy transfer process involves in STE emission in BSB:Tb^{3+}, and examine the influence of temperature on the energy transfer, we have the temperature dependent PL spectra for a 1% Tb^{3+}-doped BSB sample and presented the results in Fig. 7. In the whole temperature range (15–295 K) under study, the PL spectra of BSB:1%Tb^{3+} are composed of a broad emission band from STE and line emissions from Tb^{3+}. As the temperature drops, the original almost quenched STE emission at room temperature increases in intensity and is again clearly observed. In the meantime, the emission intensity of Tb^{3+} is gradually decreased. These observations suggest that the efficiency of the host-to-Tb^{3+} energy transfer decreased with temperature cooling and implies that the energy transfer is inhibited at low temperatures. On one hand, it is generally recognized that due to efficient energy transfer, the excitation energy will migrate about large number of centers before being emitted.[24] However, at low temperature, in the case of 1% Tb^{3+} doping, it is statistically unlikely that the STE center would be created close to a Tb^{3+} ion. In addition, as the temperature drops, it is likely that the STE is getting less mobile and even become immobilized at low temperature; as a consequence, the STE migration rate is slow down and the STE migration range is getting smaller either,[26,27]causing the energy transfer rate to Tb^{3+} is sufficiently reduced at low temperature. On the other hand, even for the purest crystals, there is always a certain concentration of defects that can act as acceptors, so that the STE emission could transfer energy to them either. These defects can relax to their ground state by multiphonon emission, and in this situation, the STE emission will be quenched either. Similar to the discussion on temperature dependent host-to-Tb^{3+} energy transfer, energy transfer efficiency from STE emission to these defects will be deceased with decreasing temperature, and therefore the intensity of the STE emission increased with decreasing temperature.

3.5 Luminescence performance comparison between BSB:Tb^{3+} and Zn_2SiO_4:Mn^{2+} and $LaPO_4$:Ce^{3+},Tb^{3+}

To further evaluate the luminescence performance of BSB:Tb^{3+}, we have compared the PL and PLE spectra, and the CIE coordinates of BSB:20%Tb^{3+} with those of Zn_2SiO_4:Mn^{2+} (P1-G1S, Kasei Optonix Ltd.) and $LaPO_4$:Ce^{3+},Tb^{3+} (NP-220, Nichia Ltd.) (see Fig. 8 and Fig. 9). The Zn_2SiO_4:Mn^{2+} phosphor is the most commonly used green-emitting phosphor in PDPs, and the $LaPO_4$:Ce^{3+},Tb^{3+} phosphor is a typical green-emitting phosphor

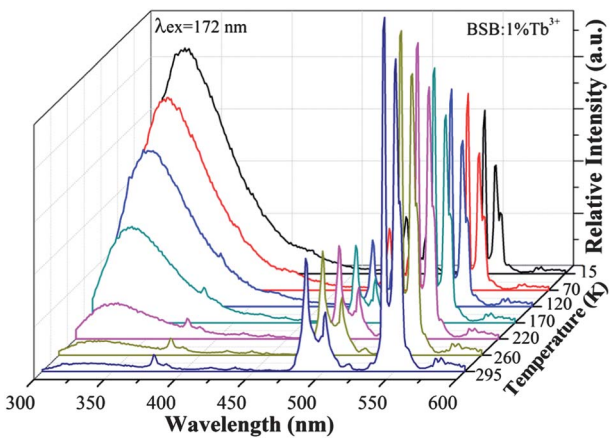

Fig. 7 Temperature dependent PL spectra of BSB:1%Tb^{3+} (λ_{ex} = 172 nm).

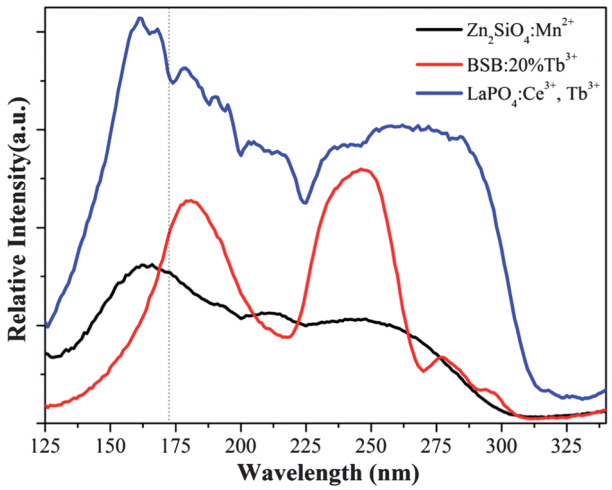

Fig. 8 Comparison of PLE spectra of BSB:20%Tb^{3+} (λ_{em} = 543 nm), commodities Zn_2SiO_4:Mn^{2+} (λ_{em} = 525 nm) and $LaPO_4$:Ce^{3+},Tb^{3+} (λ_{em} = 543 nm).

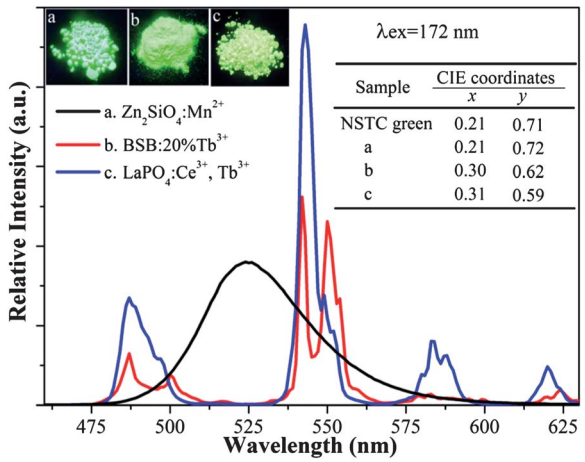

Fig. 9 PL spectra of BSB:20%Tb^{3+} and commodities Zn_2SiO_4:Mn^{2+} and $LaPO_4$:Ce^{3+},Tb^{3+} excited at 172 nm. The inset figures are the photographs the three phosphors under 254 nm UV lamp radiation, and the inset table is the CIE coordinates of the three phosphors.

widely used in CCFL. The results indicate that the PLE intensity of BSB:20%Tb^{3+} at 172 nm is about 1.25 times of that of Zn_2SiO_4:Mn^{2+}, and 58% of that of $LaPO_4$:Ce^{3+}, Tb^{3+}, respectively. Upon excitation at 172 nm, the integrated emission intensity of BSB:20%Tb^{3+} in the 470–630 nm range is about 45% of that of Zn_2SiO_4:Mn^{2+}, and 65% of that of $LaPO_4$:Ce^{3+}, Tb^{3+}, respectively. Comparing with the green CIE coordinates defined by NSTC (see the inset table in Fig. 9), it is found that BSB:20% Tb^{3+} has an inferior green color purity than that of Zn_2SiO_4:Mn^{2+}(P1-G1S), but a superior green color purity than that of $LaPO_4$:Ce^{3+},Tb^{3+}(NP-220), which is consistent with what is reflected in the inset figures in Fig. 9. In addition, heating the phosphors up to 500 °C to seal the PDP panels is inevitable, and is also essential for good adhesion between phosphor and substrate, and for complete elimination of organic additives.[28] To examine the thermal stability of BSB:Tb^{3+}, we have post-annealed the 20%-Tb^{3+} doped sample at 500 °C in the air for 3 h, then cool it down naturally to room temperature. Under 172 nm excitation, the emission intensity of the sample with post-annealing is around 95% of that without post-annealing, suggesting Tb^{3+} is quite stable in BSB:Tb^{3+}.

4 Conclusions

In summary, we have investigated the VUV-excited luminescence of the pristine- and Tb^{3+}-doped $Ba_3Sc(BO_3)_3$, and demonstrated the sensitization of Tb^{3+} emission by energy transfer from the self-trapped exciton. We also examined the influence of temperature and Tb^{3+} doping concentration on the host-to-Tb^{3+} energy transfer in $Ba_3Sc(BO_3)_3$:Tb^{3+}. Upon host excitation, $Ba_3Sc(BO_3)_3$ exhibited a broad UV emission that is attributed to the recombination of self-trapped excitons. From the excitation spectrum of the STE emission, the band gap of $Ba_3Sc(BO_3)_3$ can be roughly estimated to be about 6.9 eV. When Tb^{3+} ions were incorporated into $Ba_3Sc(BO_3)_3$, an efficient energy transfer from the host excitations to Tb^{3+} *via* STE emission was observed. The strong quenching of STE emission and similar excitation spectra of the Tb^{3+}-doped and undoped samples gave conclusive evidence for such energy transfer. In addition, it has demonstrated that host-to-Tb^{3+} energy transfer efficiency will be increased by increasing Tb^{3+} concentration and reduced by cooling temperature. As the Tb^{3+} doping concentration increases, the distance between the STE and Tb^{3+} is shortened consequently, thus the energy transfer probability is increased; while as the temperature drops, the STE is getting less mobile, as a consequence, the STE migration rate slows down and the STE migration range is getting shorter, leading to an observed reduction of energy transfer rate to Tb^{3+} at low temperature.

Acknowledgements

We gratefully thank the National Science Council of Taiwan for financial support under Contract Nos. NSC100-2811-M-009-068 (D.-Y. W.) and NSC98-2113-M-009-005-MY3 (T.-M. C.), and the group members in Dr B.-M. Cheng's Laboratory at NSRRC for their assistance with the VUV spectra measurements.

Notes and references

1 R. T. Wegh, H. Donker, K. D. Oskam and A. Meijerink, *Science*, 1999, **283**, 663.
2 C. H. Huang, T. M. Chen and B. M. Cheng, *Inorg. Chem.*, 2011, **50**, 6552.
3 K. V. Ivanovskikh, A. Meijerink, F. Piccinelli, A. Speghini, C. Ronda and M. Bettinelli, *J. Lumin.*, 2010, **130**, 893.
4 W. B. Im, Y. Kim, H. S. Yoo and D. Y. Jeon, *Inorg. Chem.*, 2009, **48**, 557.
5 D. Y. Wang, N. Kodama and L. Zhao, *J. Electrochem. Soc.*, 2010, **157**, J233.
6 L. Beauzamy, B. Moine, R. S. Meltzer, Y. Zhou, K. J. Kim and P. Gredin, *Phys. Rev. B*, 2008, **78**, 184302.
7 M. B. Xie, Y. Tao, Y. Huang, H. B. Liang and Q. Su, *Inorg. Chem.*, 2010, **49**, 11317.
8 S. Kubota and M. Shimada, *Appl. Phys. Lett.*, 2002, **81**, 2749.
9 R. L. Rabinovitz, K. J. Johnston and A. L. Diaz, *J. Phys. Chem. C*, 2010, **114**, 13884.
10 I. Y. Jung, Y. Cho, S. G. Lee, S. H. Sohn, D. K. Kim, D. K. Lee and Y. M. Kweon, *Appl. Phys. Lett.*, 2005, **87**, 191908.
11 Z. F. Tian, H. B. Liang, W. P. Chen, Q. Su, G. B. Zhang and G. T. Yang, *Opt. Express*, 2009, **17**, 956.
12 T. Jüstel, J. C. Krupa and D. U. Wiechert, *J. Lumin.*, 2001, **93**, 179.

13 C. H. Kim, I. E. Kwon, C. H. Park, Y. J. Hwang, H. S. Bae and B. Y. Yu, *J. Alloys Compd.*, 2000, **311**, 33.
14 S. X. Zhang, *IEEE Trans. Plasma Sci.*, 2006, **34**, 294.
15 B. Moine and G. Bizarri, *Opt. Mater.*, 2006, **28**, 58.
16 N. Yokosawa, K. Suzuki and E. Nakazawa, *Jpn. J. Appl. Phys.*, 2003, **42**, 5656.
17 D. L. Dexter, *J. Chem. Phys.*, 1953, **21**, 836.
18 C. J. Duan, J. L. Yuan and J. T. Zhao, *J. Solid State Chem.*, 2005, **178**, 3698.
19 H. C. Lu and B. M. Cheng, *Anal. Chem.*, 2011, **83**, 6539.
20 J. R. Cox, D. A. Keszler and J. F. Huang, *Chem. Mater.*, 1994, **6**, 2008.
21 S. P. Feofilov, Y. Zhou, J. Y. Jeong, D. A. Keszler and R. S. Meltzer, *J. Lumin.*, 2007, **125**, 80.
22 I. N. Ogorodnikov, V. A. Pustovarov, A. V. Kruzhalov, L. I. Isaenko, M. Kirm and G. Zimmerer, *Phys. Solid State*, 2000, **42**, 464.
23 C. H. Hsu and C. H. Lu, *J. Mater. Chem.*, 2011, **21**, 2932.
24 B. Henderson and G. F. Imbusch, Optical Spectroscopy of Inorganic Solids, 1989.
25 G. C. Kim, H. L. Parka and T. W. Kim, *Mater. Res. Bull.*, 2001, **36**, 1603.
26 K. Tanimura and N. Itoh, *Nucl. Instrum. Methods Phys. Res., Sect. B*, 1988, **32**, 211.
27 J. Krupa and N. A. Kulagin, *Physics of Laser Crystals*, V.126, Kluwer Academic Publishers, The Netherlands, 2002.
28 K. S. Sohn, S. S. Kim and H. D. Park, *Appl. Phys. Lett.*, 2002, **81**, 1759.

